Yoshioka, S., Torii, Y., Riedel, M. R. (2015): Impact of phase change kinetics on the Mariana slab within the framework of 2-D mantle convection. - *Physics of the Earth and Planetary Interiors*, *240*, pp. 70—81.

DOI: http://doi.org/10.1016/j.pepi.2014.12.001

Physics of the Earth and Planetary Interiors xxx (2014) xxx–xxx

Contents lists available at ScienceDirect

Physics of the Earth and Planetary Interiors

journal homepage: www.elsevier.com/locate/pepi

Impact of phase change kinetics on the Mariana slab within the framework of 2-D mantle convection

Shoichi Yoshioka [a,*], Yoku Torii [b], Michael R. Riedel [c]

[a] Research Center for Urban Safety and Security, Kobe University, Rokkodai-cho 1-1, Nada Ward, Kobe 657-8501, Japan
[b] Hewlett-Packard Development Company, Shin-Osaka Trust Tower, Miyahara 3-5-36, Yodogawa Ward, Osaka 532-0003, Japan
[c] GeoForschungsZentrum Potsdam, Telegrafenberg, 14473 Potsdam, Germany

ARTICLE INFO

Article history:
Received 8 April 2014
Received in revised form 25 September 2014
Accepted 2 December 2014
Available online xxxx

Keywords:
Temperature
Slab
Phase transformation
Kinetics
Mariana slab
Water content

ABSTRACT

Recent high-pressure and high-temperature experiments indicate that metastable olivine might persist in the cold core of a slab due to the low reaction rate of the olivine–wadsleyite phase transformation. Recent seismological observations detected a metastable olivine wedge that survives to a depth of 630 km in the Mariana slab. To consider the problem of non-equilibrium phase transformation, we developed a two-dimensional (2-D) Cartesian numerical code that incorporates the effects of kinetics into a thermal convection model. We consider the kinetics of the 410-km olivine–wadsleyite and the 660-km ringwoodite–Pv + Mw phase transformations, including the effects of water content at the 410-km phase boundary. The latent heat release of the 410-km non-equilibrium phase transformations inside the slab is also considered. The results show positive correlations between some of the controlling parameters and the length of the metastable olivine wedge: the faster the subducting velocity, and the lower the water content, the deeper is the metastable olivine wedge. With increasing depth of phase transformation, the effect of latent heat release is enhanced: heating of, at most, 100 °C occurs if olivine transforms into wadsleyite at depths greater than 570 km. Temperature increase due to the latent heat released stimulates further phase transformation, resulting in further temperature increase, acting as a positive feedback effect. We also attempt to explain the seismological observations by calculating the temperature and phase structures in the Mariana slab. If we assume that the age of the Mariana slab is 150 Myr, the subduction velocity is 9.5 cm/yr, phase transformation occurs from the grain boundary of the parental phase, and the water content is 250 wt. ppm for a grain size of 1 mm, 300 wt. ppm for one of 5 mm, and 100 wt. ppm for intracrystalline transformation, then the metastable olivine wedge survives to a depth of 630 km, which is in good agreement with the seismological observations. This suggests that the deeper portion of the Mariana slab is relatively dry. Assuming that the depression of the 660-km discontinuity by ~20–30 km within the Mariana slab, as is indicated by seismological observation, is explained by a combination of the depression caused by a negative Clapeyron slope in the cold slab and that due to the kinetics of the 660-km phase transformation, we obtain a gentle Clapeyron slope of −0.9 MPa/K for the phase transformation from ringwoodite to Pv + Mw.

1. Introduction

Phase transformation boundaries exist at depths of 410 and 660 km in the mantle between olivine, which is one of the major mineral constituents of the Earth's mantle, and its high-pressure polymorphs. Because the olivine–wadsleyite phase transformation at a depth of 410 km has a positive Clapeyron slope (e.g., Katsura and Ito, 1989), it is considered that the phase boundary is uplifted inside a low-temperature subducting oceanic plate.

However, according to high-pressure and high-temperature experiments (e.g., Sung and Burns, 1976; Rubie et al., 1990) and numerical modeling based on such experiments (Rubie and Ross, 1994; Däßler and Yuen, 1996; Däßler et al., 1996; Riedel and Karato, 1996, 1997; Kirby et al., 1996; Yoshioka et al., 1997; Devaux et al., 1997, 2000; Guest et al., 2004), because the phase transformation reaction is slow, and phase transformation is delayed in a low-temperature slab, a metastable olivine wedge may exist in the deeper parts of slabs. Mosenfelder et al. (2001) calculated the metastable area of olivine using experimentally determined kinetic data. They concluded that a metastable wedge could not persist to a depth of 600 km even in the coldest slabs,

* Corresponding author. Tel./fax: +81 78 803 6598.
E-mail address: yoshioka@port.kobe-u.ac.jp (S. Yoshioka).

http://dx.doi.org/10.1016/j.pepi.2014.12.001
0031-9201/

such as the Tonga slab, and the area of the metastable wedge would decrease if the intracrystalline transformation of the higher pressure phase was taken into account. Marton et al. (2005) calculated the phase distributions inside a slab, taking account of temperature–pressure-dependent thermal conductivity and radiation, and suggested that a metastable olivine wedge could reach a depth of at most 550 km. However, these numerical models are thermokinetic coupling models, and the momentum equation, which seriously affects the temperature field, is not solved. Numerical models to deal with the kinetics that solve the momentum and energy equations simultaneously have been proposed (e.g., Schmeling et al., 1999; Tetzlaff and Schmeling, 2000). However, olivine metastability was introduced by constant temperature in a *P–T* diagram. As a result, depth-dependent temperature and latent heat release related to the olivine–wadsleyite phase transformation are not properly incorporated into their model without solving the kinetic equation.

On the other hand, because the phase transformation associated with ringwoodite to perovskite (Pv) + magnesiowüstite (Mw) has a negative Clapeyron slope (e.g., Ito and Takahashi, 1989), the 660-km phase boundary is considered depressed inside the slab. To understand the dynamics of the upper and lower mantle interaction, it is essential to estimate the value of the Clapeyron slope correctly, although values are still controversial. High *P–T* experiments (Katsura et al., 2003; Fei et al., 2004; Litasov et al., 2005) have suggested that the phase transformation at the 660-km phase boundary has a gentle Clapeyron slope (~ −1.0 MPa/K). On the other hand, values of −2.6 MPa/K and −2.9 to −2.6 MPa/K have been suggested based on calorimetric (Akaogi et al., 2007) and first-principle calculations (Yu et al., 2007), respectively. Based on the seismologically obtained depression of the 660-km boundary and numerical calculations of the thermal structures of slabs, values of −0.7, −1.3 MPa/K, and a significantly larger absolute value have been indicated by studies of the deeper portions of the Mariana (Kubo et al., 2009), Pacific (Kawakatsu and Yoshioka, 2011), and Tonga (Kaneshima et al., 2012) slabs, respectively.

In this study, we incorporate the effects of the kinetics associated with non-equilibrium phase transformation of olivine to wadsleyite (or ringwoodite) into a conventional numerical model for thermal convection. In other words, we present a numerical model of subduction of an oceanic plate with an arbitrary shape, in which temperature, flow velocity, and degree of phase transformation can be obtained as a time-marching problem, by solving the coupled momentum, energy, and kinetics equations simultaneously. We also incorporate the kinetics associated with ringwoodite to perovskite + magnesiowüstite at the 660-km boundary, using the equation for its reaction rate obtained in a high *P–T* experiment (Kubo et al., 2002). Therefore, all of the problems, including the effect of the 410-km latent heat release, are solved in a self-consistent manner. Although a similar approach was published by Tetzlaff and Schmeling (2009), we present a formula to address the effects of water content in the kinetic equation. Recent high *P–T* experiments clearly indicate that phase reaction rate changes dramatically depending on the water content of the minerals (Kubo et al., 2004; Hosoya et al., 2005; Diedrich et al., 2007). Therefore, it is thought that the length of a metastable olivine wedge is strongly dependent on the water content of the slab. The focus of this paper is a more detailed treatment of the phase transformation kinetics, taking into account the effects of water content and its feedback effects in a subduction zone environment.

We applied our numerical model to the Mariana slab, and compared calculated phase structures in the Mariana slab with those obtained from seismological analyses, as has been done for the deeper portion of the Pacific slab (Kawakatsu and Yoshioka, 2011). Based on these experiments and the deepest possible position of a metastable olivine wedge inside the Mariana slab, Kubo et al. (2009) suggested the existence of an insignificant amount of water (150 wt. ppm) for intracrystalline transformation. Based on the notion that the depression of the 660-km phase boundary inside the Mariana slab consists of a thermal anomaly and overpressure needed for nucleation of the high-pressure phase, they also suggested a gentle value for the Clapeyron slope (−0.7 MPa/K) for the 660-km boundary. This paper is a follow up to the study of Kubo et al. (2009). The major difference is that the slab temperature is calculated based on the so-called plate cooling model, and that the water content and the value of the Clapeyron slope are obtained in a self-consistent manner without assuming latent heat release values associated with non-equilibrium phase transformation from metastable olivine to wadsleyite (or ringwoodite) and the overpressure for nucleation associated with the phase transformation from ringwoodite to Pv + Mw.

2. Method and model to calculate temperature inside a deep slab incorporating the kinetics of phase transformations

2.1. Momentum and energy equations

In this study, we assumed an incompressible fluid and disregarded an inertia term, considering the high viscosity of the mantle material. The momentum equation for a two-dimensional (2-D) Cartesian box model (Christensen and Yuen, 1985) is given by:

$$\frac{\partial^2}{\partial x \partial z}\left[4\eta\frac{\partial^2\psi}{\partial x\partial z}\right]+\left(\frac{\partial^2}{\partial z^2}-\frac{\partial^2}{\partial x^2}\right)\left[\eta\left(\frac{\partial^2}{\partial z^2}-\frac{\partial^2}{\partial x^2}\right)\psi\right] = -\frac{\partial}{\partial x}(\rho_0 g\alpha T), \quad (1)$$

where x and z are horizontal and vertical coordinates, respectively, ψ is stream function, ρ_0 is the standard density for the upper mantle, g is the acceleration of gravity, α is thermal expansivity with a constant value, and T is temperature. Viscosity η is dependent on temperature and depth (Christensen, 1996), which is given by:

$$\eta = \eta_0 \exp\left(\frac{T_0 - T}{a} + \frac{z}{b} - \left(\frac{z}{c}\right)^2\right), \quad (2)$$

where η_0 is the coefficient of viscosity, T_0 is the potential temperature for the mantle, and a, b, and c are constants. Using the horizontal and vertical velocities u and v, respectively, ψ is defined by:

$$u = \frac{\partial\psi}{\partial z}, \quad v = -\frac{\partial\psi}{\partial x} \quad (3)$$

Using the extended Boussinesq approximation, the dimensionless energy equation can be represented by:

$$\frac{DT}{Dt} = \nabla^2 T + (T + T_s)Di\mathbf{v} + \frac{Di}{Ra}\sigma_{ij}\frac{\partial u_i}{\partial x_j} + Q, \quad (4)$$

with

$$\frac{D}{Dt} = \frac{\partial}{\partial t} + \mathbf{v}\cdot\nabla, \quad (5)$$

where T_s is the temperature at the model surface, t is time, Di is the dissipation number, $\mathbf{v}$ is the flow velocity vector, Ra is the Rayleigh number, σ_{ij} is the stress tensor, u_i is the flow velocity component, and x_j is the coordinate component. In this study, constant thermal conductivity is assumed. The first, second, third, and fourth terms on the right-hand side of Eq. (4) represent the thermal conduction, adiabatic compression, viscous dissipation, and latent heat release associated with phase transformation, respectively. Because the temperature inside the slab is low, taking into account non-equilibrium olivine–wadsleyite phase transformation, the latent heat term Q can be represented by:

Please cite this article in press as: Yoshioka, S., et al. Impact of phase change kinetics on the Mariana slab within the framework of 2-D mantle convection. Phys. Earth Planet. In. (2014), http://dx.doi.org/10.1016/j.pepi.2014.12.001

$$Q = F_{ol}\frac{\Delta Q}{\rho C_p \Delta T}\frac{D\xi}{Dt}, \tag{6}$$

where F_{ol} is the volume fraction of olivine, ρ is the density, C_p is the specific heat at constant pressure, ΔT is the temperature difference between the top and bottom boundaries of the model, and ξ is the degree of phase transformation. The latent heat release ΔQ associated with a non-equilibrium phase transformation (Däßler et al., 1996) is represented by:

$$\Delta Q = \Delta H_{T,equ} + \int_{P_{equ}}^{P} \Delta V(P',T)dP' \tag{7}$$

For simplicity, the volume change $\Delta V(P',T)$ associated with phase transformation is assumed constant irrespective of pressure and temperature. $\Delta H_{T,equ}$ is the latent heat for equilibrium phase transformations, which is given by:

$$\Delta H_{T,equ} = T\Delta S, \tag{8}$$

where ΔS is the entropy change. The degree of phase transformation ξ will be explained in detail in the next section.

The momentum Eq. (1) and the energy Eq. (4) are solved simultaneously as a coupled problem, using the finite difference method (Andrews, 1972; Takami and Kawamura, 1994).

2.2. Kinetic equation

This section describes the method used to calculate the degree of phase transformation ξ. In the initial stage, phase transformation is dominated by the nucleation and growth of the grains of the lower-pressure mineral. The grains of the new, higher-pressure phase are produced along the grain boundaries of the parental phase. This process is described by the nucleation rate $I(P,T)$. Then, the size of each of these new grains increases. This process is described by the growth rate $Y(P,T)$. Once site saturation is reached at the grain boundaries of the parental phase, nucleation ceases, and the phase transformation proceeds only by the growth process. The dimensionless time τ_s to reach site saturation (Cahn, 1956) is given by:

$$\tau_s = \frac{\kappa}{D^2}\left(\frac{I(P,T)Y(P,T)^2 d_0}{6.7}\right)^{-\frac{1}{3}}, \tag{9}$$

where κ is the thermal diffusivity, D is the thickness of the slab, and d_0 is the grain size of olivine.

The grain boundary nucleation rate $I(P,T)$ (Christian, 1975) is represented by the following equation:

$$I(P,T) = K_0 T\ \exp\left(\frac{-\phi\Delta G^*_{\hom}}{kT}\right)\ \exp\left(\frac{-Q_a}{RT}\right) \tag{10}$$

with

$$\Delta G^*_{\hom} = \frac{16\pi\gamma^3}{3(\Delta G_v + \varepsilon)^2}, \tag{11}$$

and

$$Q_a = \Delta H_a + PV^*, \tag{12}$$

where K_0 is a constant, ϕ is the shape factor, $\Delta G^*_{\hom}$ is the activation energy for homogeneous nucleation, k is the Boltzmann constant, Q_a is the activation energy for growth, R is the gas constant, γ is the surface energy, ΔG_v is the free energy change per volume, ε is the strain energy, which is assumed to be 0, and V^* is the activation volume.

On the other hand, the water-content-dependent growth rate $Y(P,T)$ for the olivine–wadsleyite transformation (Hosoya et al., 2005) is given by:

$$Y(P,T) = ATC_{OH}^n \exp\left(-\frac{\Delta H_a + PV^*}{RT}\right)\left[1 - \exp\left(\frac{-\Delta G_r}{RT}\right)\right], \tag{13}$$

with

$$\Delta G_r = \Delta P \times \Delta V. \tag{14}$$

For the growth rate in the phase transformation associated with ringwoodite to perovskite + magnesiowüstite, we used the following equation by Kubo et al. (2002):

$$Y(P,T) = K'\Delta G_v^2\ \exp(-Q/RT), \tag{15}$$

where A and K' are constants, C_{OH} is the water content, n is the exponent of C_{OH}, ΔH_a is the activation enthalpy, ΔG_r is the free energy change per mol associated with the phase transformation, and ΔP is the excess pressure from an equilibrium phase transformation. The numerical values used for each parameter are given in Table 1. It should be noted that in this study we assume that the kinetics of olivine to ringwoodite is the same as that of olivine to wadsleyite, and that the nucleation kinetics of Pv + Mw is identical to that of olivine to wadsleyite because such kinetics are still unknown.

Before reaching the state of site saturation ($\tau \le \tau_s$), phase transformation proceeds with homogeneous nucleation. The degree of phase transformation ξ (Däßler et al., 1996) can be calculated from:

$$\xi = 1 - \exp(-X_3(\tau)), \tag{16}$$

with

$$\tau = \frac{t}{\left(\frac{D^2}{\kappa}\right)}, \tag{17}$$

where τ is the dimensionless time. $X_3(\tau)$ can be obtained by solving the following four coupled ordinary differential equations:

$$\frac{d}{d\tau}\begin{bmatrix} X_3(\tau) \\ X_2(\tau) \\ X_1(\tau) \\ X_0(\tau) \end{bmatrix} = \sqrt[4]{Av}\begin{bmatrix} 0 & 4\pi Y^*(\tau) & 0 & 0 \\ 0 & 0 & 2Y^*(\tau) & 0 \\ 0 & 0 & 0 & Y^*(\tau) \\ 0 & 0 & 0 & 0 \end{bmatrix}\begin{bmatrix} X_3(\tau) \\ X_2(\tau) \\ X_1(\tau) \\ X_0(\tau) \end{bmatrix} + \sqrt[4]{Av}\begin{bmatrix} 0 \\ 0 \\ 0 \\ I^*(\tau) \end{bmatrix}, \tag{18}$$

where $X_3(\tau)$, $X_2(\tau)$, $X_1(\tau)$, and $X_0(\tau)$ are the total grain volume, total grain area, total grain diameter, and number of grains, respectively (Avrami, 1941). $I^*(\tau)$ and $Y^*(\tau)$ are the dimensionless nucleation and growth rates, respectively. The Avrami number Av is a dimensionless number indicating the ratio between the timescale of thermal diffusion and that of kinetics during the transformation processes (Spohn et al., 1988), which is defined by:

$$A_v = \left(\frac{D^2}{\kappa}\right)^4 I_{\max}(P,T)Y_{\max}(P,T)^3, \tag{19}$$

where $I_{\max}(P,T)$ and $Y_{\max}(P,T)$ are the maximum nucleation and growth rates, respectively. The ranges of Av for the olivine–wadsleyite and the ringwoodite–Pv + Mw phase transformations estimated in this study are too large. This indicates that the heat-diffusion timescale is much larger than the kinetic timescale.

After reaching the state of site saturation ($\tau \ge \tau_s$), nucleation ceases, and the growth process becomes dominant. In this case, the degree of phase transformation ξ is dependent only on the growth rate, not the nucleation rate. Following Cahn (1956) and Yoshioka et al. (1997), ξ is expressed as:

Please cite this article in press as: Yoshioka, S., et al. Impact of phase change kinetics on the Mariana slab within the framework of 2-D mantle convection. Phys. Earth Planet. In. (2014), http://dx.doi.org/10.1016/j.pepi.2014.12.001

Table 1
Model parameters given in this study.

Parameter related to model	Symbol	Value	Unit
Standard density for the mantle	ρ_0	3300[a]	kg/m^3
Acceleration of gravity	g	9.8	m/s^2
Potential temperature	T_0	1350[b]	°C
Thermal expansivity	α	2.0×10^{-5}[c]	K^{-1}
Thermal conductivity	k	4.184[d]	J/(m K s)
Specific heat at constant pressure	C_p	1046[d]	kJ/(kg K)
Temperature difference between top and bottom of the model	ΔT	1624	K
Volume fraction of olivine	F_{ol}	0.6[e]	
Parameter related to viscosity[f]			
	η_0	1×10^{21}	Pa s
	a	131.3[f]	K
	b	165×10^3	km
	c	1086×10^3[f]	km
Parameter related to the olivine to wadsleyite phase transformation[g]			
Clapeyron slope		3[h]	MPa/K
Entropy difference	ΔS	5.97	J/(mol K)
Volume change	ΔV	2.1×10^{-6}	m^3/mol
Phase transformation pressure at 0 K	p_0	8.69	GPa
Grain size of parental olivine	d_0	1, 5	mm
Parameter related to the ringwoodite to Pv + Mw phase transformation[g]			
Clapeyron slope		−1[i], −0.9	MPa/K
Volume change	ΔV	1.08×10^{-6}	m^3/mol
Phase transformation pressure at 0 K	p_0	27.77	GPa
Grain size of parental ringwoodite	d_0	1	mm
Parameter related to nucleation rate[j]			
Pre-exponential factor	K_0	3.54×10^{38}	s^{-1} m^{-2} K^{-1}
Shape factor and interfacial energy	$f^{1/3}g$	0.0506	J/m^2
Activation volume	V^*	4×10^{-6}	cm^3/mol
Activation enthalpy	ΔH_a	344×10^3	J/mol
Parameter related to growth rate for the olivine–wadsleyite transformation[k]			
Pre-exponential factor	ln A	−18	m/s
Water-content exponent	n	3.2 ± 0.6	
Activation volume	V^n	$3.3 \pm 3.8 \times 10^{-6}$	cm^3/mol
Activation enthalpy	ΔH_a	274 ± 87	kJ/mol
Parameter related to growth rate for the ringwoodite–Pv + Mw transformation[l]			
Pre-exponential factor	K'	8.11	s^{-1} m^{-2} K^{-1}
Activation energy	Q	355	kJ/mol

[a] Wang et al. (1995).
[b] Takenaka et al. (1999).
[c] Honda (1997).
[d] Yoshioka and Sanshadokoro (2002).
[e] Riedel and Karato (1997).
[f] Christensen (1996).
[g] Yoshioka et al. (1997).
[h] Katsura and Ito (1989).
[i] Katsura et al. (2003), Fei et al. (2004).
[j] Rubie et al. (1990), Rubie and Ross (1994).
[k] Hosoya et al. (2005).
[l] Kubo et al. (2002).

$$\xi = 1 - \exp\left(-\frac{6.7D^2}{d_0\kappa}Y(P,T)\tau\right). \quad (20)$$

2.3. Model

In this study, based on the studies by Yoshioka and Sanshadokoro (2002) and Torii and Yoshioka (2007), we constructed a 2-D Cartesian box thermal convection model with horizontal and vertical lengths of 1200 and 1000 km, respectively (Fig. 1). A prescribed guide corresponding to a subducting oceanic plate was set, and constant subduction velocity was given in the domain occupied by the oceanic plate elongating progressively with time. We solved the temperature fields for the whole model domain and the mantle flow for the domain except for the lithosphere on the back-arc side of a trench and the slab at each time step alternatively, using the finite difference method. On the back-arc side of the trench, we set a conductive layer with a thickness of 50 km from the Earth's surface, corresponding to the lithosphere. The thickness of the subducting plate was estimated from the age of the oceanic plate at the trench using the equation of Yoshii (1975). Because the oceanic plate is forced to subduct with constant velocity along the prescribed guide to depths in the lower mantle, the differences in calculated temperatures and phase distributions inside the slab caused by using different forms of temperature- and depth-dependent equations of viscosity is negligible. In addition, because our model is not fully dynamic, the possible formation of a stagnant slab owing to the buoyancy of an untransformed, light metastable olivine wedge inside the slab (e.g., Tetzlaff and Schmeling, 2000) cannot be discussed.

An initial temperature distribution was given based on the so-called plate cooling model (Carslaw and Jaeger, 1959; Turcotte and Schubert, 2002) at depths shallower than the base of a hori-

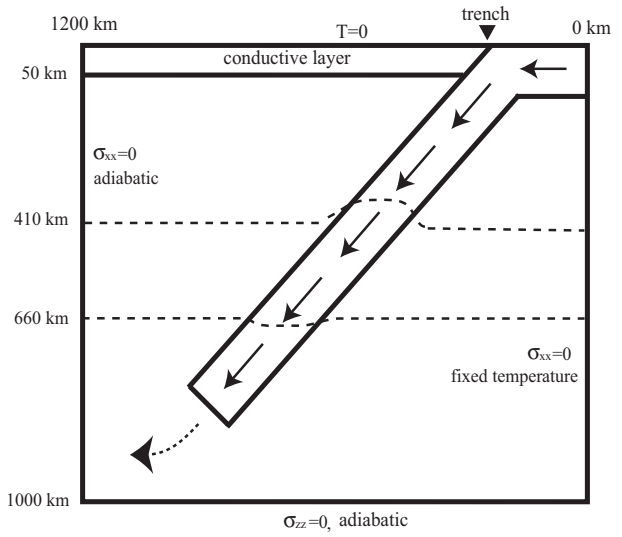

Fig. 1. Two-dimensional Cartesian box thermal convection model used in our numerical simulations to obtain temperature and flow fields and degree of phase transformation. For boundary conditions, see text.

zontal oceanic plate of 134.9 km, at which the mantle temperature is 1402 °C, using Model RT1 by Grose (2012). Adiabatic heating was considered at depths below 134.9 km (Griggs, 1972). As boundary conditions, we assumed fixed temperatures at the top and on the right boundary, taking into account subduction of the oceanic plate, and adiabatic conditions for the left and bottom boundaries. For flow conditions, normal stress was assumed to be zero for the left, right, and bottom boundaries, except for the oceanic plate on the right boundary.

3. Results and discussion

3.1. Kinetics for the olivine–wadsleyite and ringwoodite–Pv + Mw phase transformations

The phase diagram of the olivine–wadsleyite phase transformation is obtained by solving the equations described in Section 2.2 Fig. 2 shows an example of the phase diagram obtained by assuming a water content of 200 wt. ppm. In the low-temperature domain at less than about 630 °C in the phase diagram, metastable olivine is expected to exist due to the low rate of reaction of the phase transformation. It should be noted that the kinetic curves shift to the higher-temperature side with decreasing water content. So, a metastable olivine wedge inside a slab is expected to be produced more easily with decreasing water content.

We also modeled the kinetics of the ringwoodite–Pv + Mw phase transformation. Because no equation has yet been proposed for the nucleation rate of this phase transformation, we used the equation for the olivine–wadsleyite phase transformation (Rubie et al., 1990; Rubie and Ross, 1994). From the phase diagram, we found that the metastable area for the phase transformation of ringwoodite to Pv + Mw is shifted to a lower-temperature than in the olivine–wadsleyite phase transformation. Therefore, unlike the case of the 410-km phase transformation, metastable ringwoodite would not survive below the 660-km phase boundary, even considering the typical pressure–temperature path for the cold core of a slab. However, it should be noted that the 660-km phase boundary is expected to be depressed due to the effect of kinetics in addition to the effect of a thermal anomaly because overpressure is to some extent required to initiate phase transformation (Kubo et al., 2009). In addition, the growth kinetics for this transformation was examined under relatively wet conditions (~1000–2000 wt. ppm) (Kubo et al., 2008), which affects the phase diagram. The nucleation kinetics and the effects of water on the growth rate in this phase transformation need to be clarified in the future.

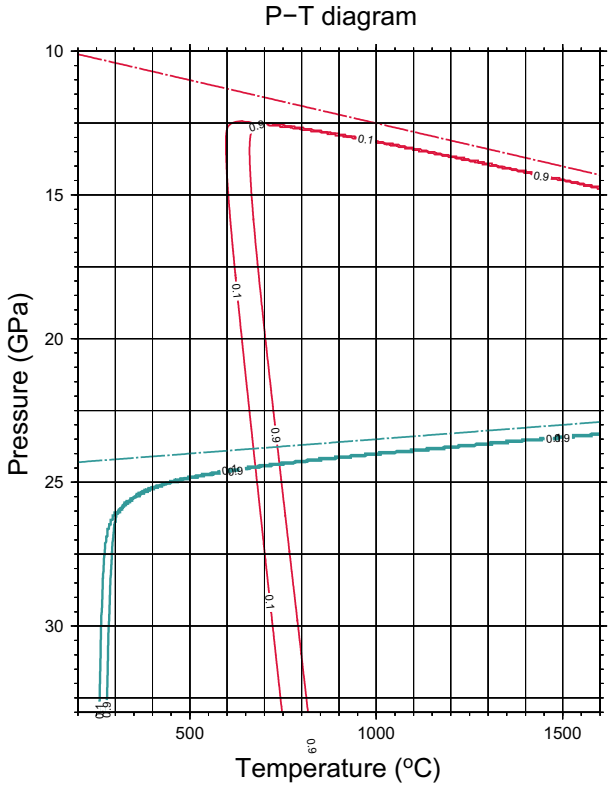

Fig. 2. Calculated phase diagrams for the olivine–wadsleyite and ringwoodite–Pv + Mw phase transformations. The red and blue dash-dotted lines denote the Clapeyron curves for the equilibrium phase transformations from olivine to wadsleyite and ringwoodite to Pv + Mw, respectively. The lines are drawn assuming Clapeyron slopes of 3 and −1.0 MPa/K, respectively. The two red and two blue lines represent degrees of phase transformation of 10% and 90% from olivine to wadsleyite and ringwoodite to Pv + Mw, respectively. The case if the water content associated with the phase transformation from olivine to wadsleyite is 200 wt. ppm is shown. It should be noted that the water content of phase transformation from ringwoodite to Pv + Mw ranges from 1000 to 2000 wt. ppm, resulting in phase transformation at a lower temperature than that from olivine to wadsleyite. (For interpretation of the references to color in this figure legend, the reader is referred to the web version of this article.)

3.2. Temperature and phase distributions associated with subduction of an oceanic plate

3.2.1. Equilibrium and non-equilibrium phase transformations from olivine to wadsleyite

In this section, we discuss the calculated temperature and phase structures in and around the slab associated with subduction of the oceanic plate. Fig. 3a shows an example of the calculated temperature field for an equilibrium phase transformation, assuming a subduction velocity of 8 cm/yr, an age for the oceanic plate at the trench and the initial age of the back-arc side of 130 Myr, and a dip angle of 45°. The values of the Clapeyron slope for the 410-km and 660-km phase transformations are assumed to be 3 and −1 MPa/K, respectively. The effect of latent heat release associated with the 410-km phase transformations is not included. The calculated results show that, as expected, the 410- and 660-km phase boundaries are uplifted and depressed, respectively, inside the slab.

Please cite this article in press as: Yoshioka, S., et al. Impact of phase change kinetics on the Mariana slab within the framework of 2-D mantle convection. Phys. Earth Planet. In. (2014), http://dx.doi.org/10.1016/j.pepi.2014.12.001

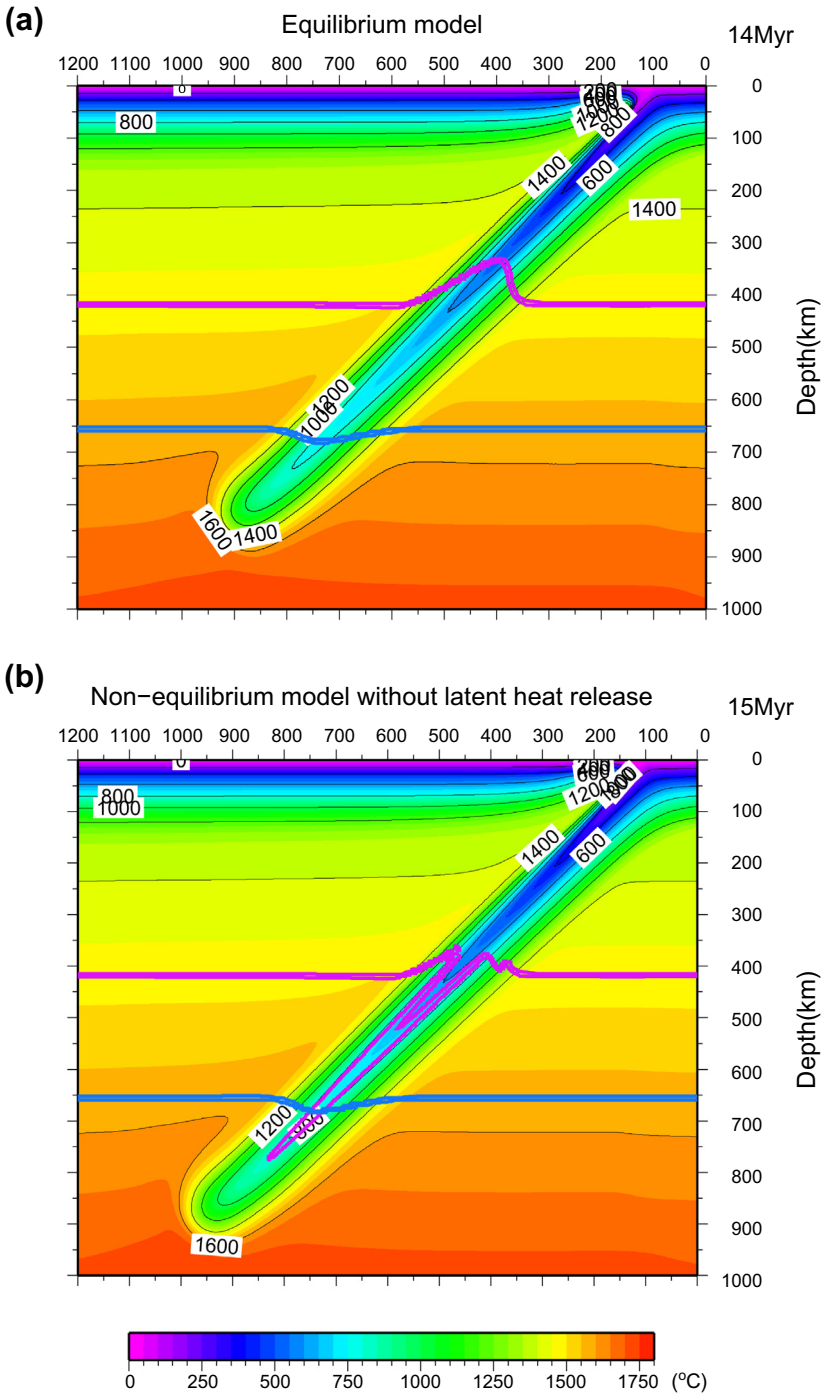

Fig. 3. Calculated temperature and phase distributions associated with subduction of the oceanic plate at 14 Myr after its initiation. The age of the oceanic plate at the trench is 130 Myr, subduction velocity is 8 cm/yr, and the dip angle is 45°. The pink and blue lines represent the calculated 410-km and the 660-km phase boundaries, respectively. The two lines for the respective colors denote degrees of phase transformation of 10% and 90%. (a) Equilibrium phase transformation for the 410-km phase transformation. Latent heat release associated with the equilibrium phase transformation is not included. There is no water content. Equilibrium phase transformation is assumed for the 660-km phase transformation, and latent heat absorption is not included. (b) Non-equilibrium phase transformation for the 410-km phase transformation. Latent heat release associated with the non-equilibrium phase transformation is not included. Water content is 50 wt. ppm. Non-equilibrium phase transformation is assumed for the 660-km phase transformation, and latent heat absorption is not included. (For interpretation of the references to color in this figure legend, the reader is referred to the web version of this article.)

If non-equilibrium phase transformation is taken into account, the phase distribution changes dramatically. Fig. 3b is the calculated temperature and phase distributions for the non-equilibrium phase transformation from olivine to wadsleyite. Although the parameter values are the same as in Fig. 3a, the water content is assumed to be 50 wt. ppm, and latent heat release associated with the phase transformation is not incorporated into the model. When the slab is old and the subduction velocity is fast, the temperature inside the slab decreases, tending to produce a metastable olivine wedge in the central part of the deep slab. In Fig. 3b, the metastable olivine wedge survives to a depth of 770 km, which is unrealistic.

Please cite this article in press as: Yoshioka, S., et al. Impact of phase change kinetics on the Mariana slab within the framework of 2-D mantle convection. Phys. Earth Planet. In. (2014), http://dx.doi.org/10.1016/j.pepi.2014.12.001

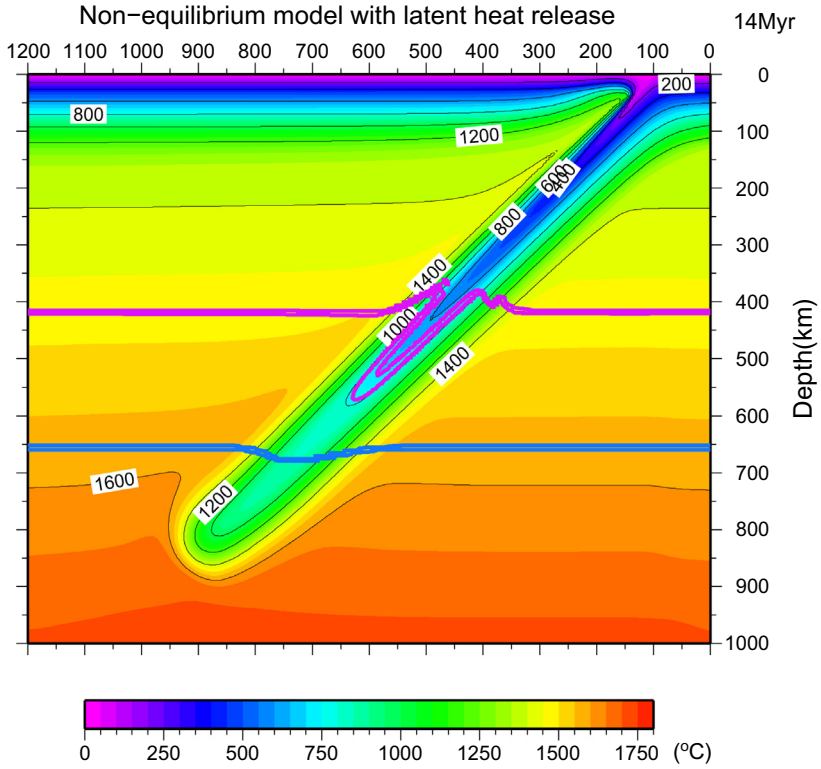

Fig. 4. The same as Fig. 3b, except that the latent heat release associated with the 410-km non-equilibrium phase transformation is included.

3.2.2. The effect of latent heat release associated with phase transformation on phase distribution

Fig. 4 shows a model in which the effect of latent heat release is added to the model shown in Fig. 3b. In Fig. 3b, the two lines of the degree of the 410-km phase transformation (ξ = 10% and ξ = 90%) depict large depth difference inside the slab, indicating that phase transformation takes place gradually from initiation to completion. On the other hand, if the latent heat release associated with the 410-km phase transformation is taken into account, the depth of completion of the olivine–wadsleyite phase transformation becomes much shallower (~570 km) (Fig. 4). The temperature in the cold core of the slab below 570 km is higher in Fig. 4 than in Fig. 3b by at most 100 °C due to the effect of latent heat release. The distance between the two lines of the degree of phase transformation in Fig. 4 is less than that in Fig. 3b, indicating that phase transformation is completed within a relatively short time. This is because, in Fig. 4, once phase transformation is initiated, further phase transformation is promoted by the temperature increase associated with the latent heat released by the phase transformation. This results in further latent heat release. Therefore, the latent heat release causes a positive feedback effect.

3.2.3. The effect of subduction velocity on phase distribution

A model in which the subduction velocity is reduced to 4 cm/yr for the Fig. 4 model is shown in Fig. 5a. In this case, because the temperature inside the slab is sufficiently high, at ~700 °C at a depth of 410 km, the appearance of only a slight metastable olivine wedge can be identified in the central part of the slab below the uplifted equilibrium phase boundary.

3.2.4. The effects of water content on phase distribution

The kinetics of the olivine–wadsleyite phase transformation is also affected by water content. Fig. 5b shows the case when the water content is assumed to be 200 wt. ppm in the Fig. 4 model. A metastable olivine wedge persists to a depth of 570 km for a water content of 50 wt. ppm (Fig. 4), whereas it barely survives when the water content is 200 wt. ppm (Fig. 5b). Therefore, the lower the water content, the greater the depth to which a metastable olivine wedge survives. Comparing the temperature distribution inside the slab for a water content of 50 wt. ppm with that for 200 wt. ppm, we found that in the central part of the slab below 570 km, the temperature is higher for the former than for the latter. This is because the temperature increase due to latent heat release associated with the 410-km non-equilibrium phase transformation is larger at greater depths than at shallower depths. This is also because the pressure dependence of latent heat release is incorporated into the model, as shown in Eq. (7) (Däßler et al., 1996).

3.3. Application to the Mariana slab

3.3.1. Water content of the Mariana slab

Based on seismological analysis, Kaneshima et al. (2007) detected a metastable olivine wedge that persisted to a depth of ~630 km in the Mariana slab. To explain the seismological observation, we applied the newly developed temperature and phase calculation code to the Mariana slab. We assumed an age of the Mariana slab at the trench and an initial age of the back-arc side of the plate of 150 Myr, a subduction velocity of 9.5 cm/yr, and the shape of the Mariana slab to be as delineated by seismic tomography (Fukao et al., 2001). As a result, if we assume a water content of 250 wt. ppm for a grain size of 1 mm, and 300 wt. ppm for one of 5 mm, the seismological observation indicating that a metastable olivine wedge exists to a depth of 630 km is well explained (Fig. 6).

High-pressure and high-temperature experiments (Kerschhofer et al., 1996, 2000) and theoretical calculations (Liu and Yund, 1995) Q3 suggest that if the olivine–ringwoodite transformation takes place at higher than 18 GPa, then nucleation takes place not only along the grain boundaries of the parental olivine, but also from within. Here, we performed a numerical simulation of this intracrystalline nucleation by incorporating this effect into our model in a simple

Please cite this article in press as: Yoshioka, S., et al. Impact of phase change kinetics on the Mariana slab within the framework of 2-D mantle convection. Phys. Earth Planet. In. (2014), http://dx.doi.org/10.1016/j.pepi.2014.12.001

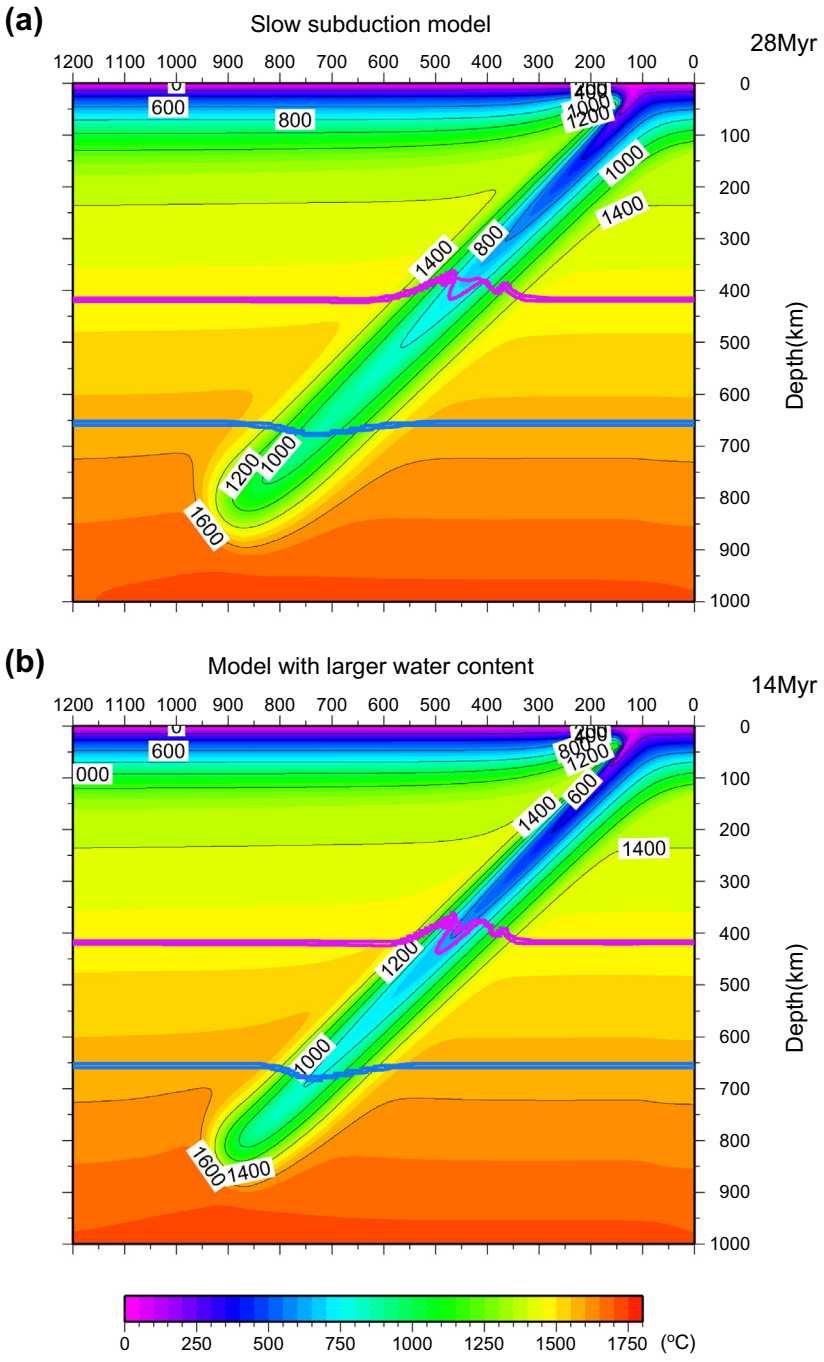

Fig. 5. (a) The same as Fig. 4, except that the subduction velocity is 4 cm/yr and the elapsed time is 28 Myr after the initiation of subduction. (b) The same as Fig. 4, except that the water content is 200 wt. ppm.

manner. Following Mosenfelder et al. (2001), we assumed that intracrystalline nucleation takes place at 18 GPa (approximately 520 km in depth), and the grain size d_0 of the parental olivine was set to be 50 μm in Eqs. (9) and (20). We found that phase transformation completes faster than that in Fig. 6 at depths greater than 520 km. In this case, the water content necessary to explain the observed depth of the metastable olivine wedge was estimated to be 100 wt. ppm.

Kubo et al. (2009) estimated the water content of the Mariana slab to be 500 wt. ppm for a grain size of 5 mm for the grain boundary nucleation model and 150 wt. ppm for intracrystalline transformation, assuming a simplified thermal structure. Therefore, the water contents estimated in this study are lower than those of Kubo et al. (2009). The differences in water contents between our work and that of Kubo et al. (2009) originate from differences in slab geometry and thermal structure. In contrast to the vertical subduction of the oceanic plate of Kubo et al. (2009), the deeper portion of our oceanic plate is subducting toward the oceanic side (Fig. 6), which is more realistic. In this study, to provide a temperature profile of the oceanic plate at the trench, we applied the so-called plate cooling model using the model parameter values given by Grose (2012), whereas a half-space cooling model was used by Kubo et al. (2009). In the case of oceanic plates over 80 Myr old, the seafloor depths and heat flows calculated using a half-space cooling model do not fit observations well. This is because an old oceanic plate is heated from the bottom and the temperature of an

Please cite this article in press as: Yoshioka, S., et al. Impact of phase change kinetics on the Mariana slab within the framework of 2-D mantle convection. Phys. Earth Planet. In. (2014), http://dx.doi.org/10.1016/j.pepi.2014.12.001

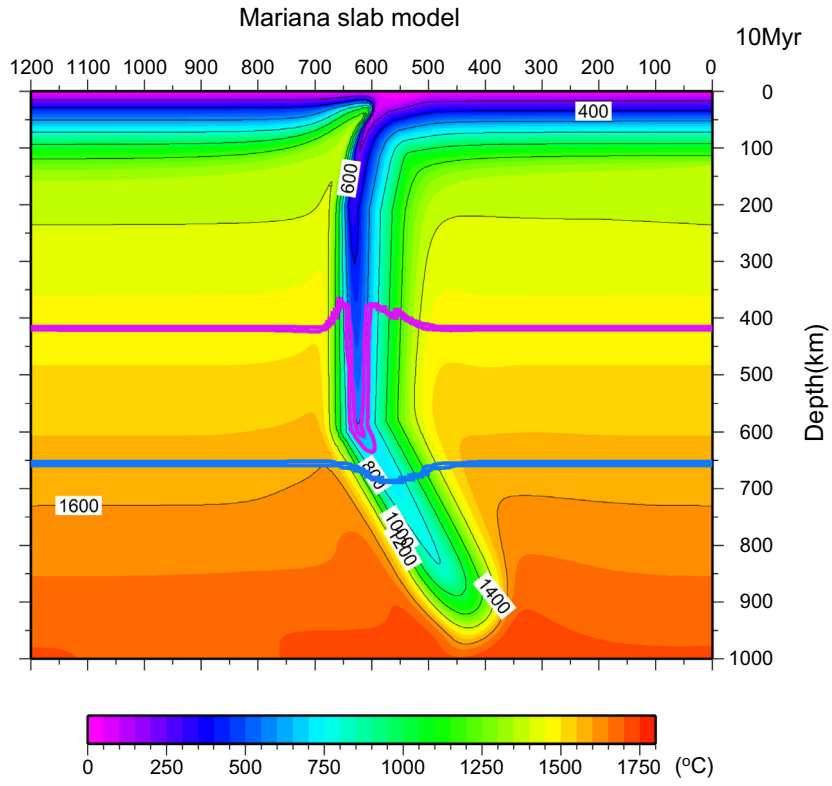

Fig. 6. Calculated temperature and phase distributions associated with the subduction of the Mariana slab at 10 Myr after its initiation. The model explains the depth of the seismologically detected metastable olivine wedge and the amount of depression of the 660-km phase boundary in the Mariana slab. The age of the oceanic plate at the trench is 150 Myr, and the subduction velocity is 9.5 cm/yr. The shape of the slab is delineated based on the results of seismic tomography (Fukao et al., 2001). The pink and blue lines represent the 410- and 660-km phase boundaries, respectively. The two lines for the respective colors denote degrees of phase transformation of 10% and 90%. Non-equilibrium phase transformations are assumed for the 410- and 660-km phase transformations. Latent heat release is included for the 410-km phase transformation, whereas latent heat absorption is not included for the 660-km phase transformation. This is the model in which nucleation takes place only along grain boundaries for a grain size of 1 mm. The estimated water content is 250 wt. ppm. The estimated value of the Clapeyron slope for the ringwoodite–Pv + Mw phase transformation is −0.9 MPa/K. (For interpretation of the references to color in this figure legend, the reader is referred to the web version of this article.)

actual plate is not low compared with the temperature calculated by the half-space cooling model (Stein and Stein, 1992). Therefore, for an old oceanic plate such as the Mariana slab, the plate cooling model is preferable to the half-space cooling model. As a result, the thermal gradient of the oceanic plate at the trench in this study, and hence the slab temperature, is greater than that reported by Kubo et al. (2009), resulting in a lower water content, as obtained in this study. In addition, in this study, temperature was obtained in a self-consistent manner, by solving the momentum, energy and kinetics equations simultaneously. The temperature increase from a depth of 600 to 660 km in the central part of the slab is ~155 °C in the model of Kubo et al. (2009), whereas it is at most 100 °C in our model. This indicates that the difference in the effective latent heat release associated with the phase transformation from olivine to wadsleyite between the two models is greater than 55 °C. In the model of Kubo et al. (2009), because of the large latent heat release, which was overestimated, a sharp phase transformation takes place at a depth of 630 km. On the other hand, some amount of depth range is needed to complete phase transformation in our model (Fig. 6).

Based on numerical modeling results for the Mariana slab, Quinteros and Sobolev (2012) suggested a blocking temperature for the olivine–wadsleyite phase transformation of ~725 °C. We do not include the concept of a constant blocking temperature, but a depth-dependent temperature for the phase transformation is adopted because we solved the realistic kinetic equation. The temperatures obtained for the phase transformation of 10% and 90% were 550–650 °C and 650–700 °C, respectively (Fig. 6).

3.3.2. Effect of uncertain model parameters on estimates of water content

Based on our numerical modeling, we estimated the water content of the Mariana slab to be 250 wt. ppm for a grain size of 1 mm. However, a result may depend on the given parameter values. In this section, we discuss the effects of the uncertainty of parameter values on the calculated results by carrying out some sensitivity tests, assuming that water content is a free parameter.

One of the uncertain parameters in this study is the thermal structure of the subducting oceanic plate. In this study, we used the plate cooling model of Grose (2012). Because the age of the Mariana slab is 150 Myr at the trench, which is sufficiently old, the thermal gradient there changes little in the plate cooling model even if the apparent age is changed to 130 or 170 Myr. Therefore, the age does not affect the obtained results. However, using the plate cooling model by Stein and Stein (1992) with an age of 150 Myr at the trench, the water content of the Mariana slab is estimated to be 30 wt. ppm. Because the thermal gradient of the oceanic plate at the trench is much larger in this plate cooling model (15.3 °C/km) than in Grose (2012) (10.4 °C/km), the slab temperature is higher. This results in a much smaller water content to produce a metastable olivine wedge to a depth of 630 km. In other words, the higher the temperature of the Mariana slab, the drier it is. We considered the Grose (2012) model is more preferable because formalisms were developed for the evaluation of the effective properties of the oceanic lithosphere and the treatment of temperature-dependent thermal conductivity and thermal expansivity as both variables and freely adjustable parameters in fitting

Please cite this article in press as: Yoshioka, S., et al. Impact of phase change kinetics on the Mariana slab within the framework of 2-D mantle convection. Phys. Earth Planet. In. (2014), http://dx.doi.org/10.1016/j.pepi.2014.12.001

analysis, and excellent fits to seafloor depth and marine heat flow were resolved for a wide range of models.

On the other hand, using a half-space cooling model with an age of 150 Myr, the thermal gradient (~9.0 °C/km) is smaller than that of Grose (2013). In this case, a larger water content of 700 wt. ppm is necessary to explain the depth of the observed metastable olivine wedge. This is because the slab is colder; accordingly the water content must be higher to produce the same depth for a metastable olivine wedge.

Some of the values of the physical properties used in the kinetic equation have some uncertainties; among them, the activation volume V^* and activation enthalpy ΔH_a values are the most uncertain. Here, we carried out sensitivity tests, assuming 10% errors in these experimentally determined values (Hosoya et al., 2005). If the value of the activation volume is 3.0 cm^3/mol, instead of using the experimentally determined value of 3.3 cm^3/mol, the water content must then be 200 wt. ppm to produce a metastable olivine wedge to a depth of 630 km in the Mariana slab. If an activation enthalpy of 247 kJ/mol is given, instead of 274 kJ/mol, then the probable water content becomes 75 wt. ppm.

It should be noted that these sensitivity tests for water content are based on a grain size of 1 mm (250 wt. ppm). Sensitivity tests for a grain size of 5 mm (300 wt. ppm) and intracrystalline transformation (100 wt. ppm) showed higher and lower water contents, respectively. The results of these sensitivity tests indicate that the water content is low, suggesting that the deeper portion of the Mariana slab is relatively dry.

3.3.3. Possible water contents of slabs

In this study, we estimated the water content of the Mariana slab based on the experimentally obtained Eq. (13) by Hosoya et al. (2005). They measured the rate of the olivine–wadsleyite phase transformation in pure forsterite Mg_2SiO_4 at high *P–T* under hydrous conditions at 660–5000 wt. ppm, and demonstrated that the growth rate in the phase transformation is proportional to water content to the power of ~3.2. They suggested that the depth at which olivine transformation occurs changes with the water content of the cold slabs, and this must be considered to estimate the fields of metastable olivine. However, it should be noted that the rate of phase transformation at a water content of less than 660 wt. ppm estimated in that study was extrapolated, not measured directly. Recently, Perrillat et al. (2013) experimentally investigated the mechanism and kinetics of olivine–wadsleyite phase transformation in San Carlos olivine $Mg_{1.8}Fe_{0.2}SiO_4$ with an approximate water content of 526 wt. ppm under high *P–T* conditions. Comparing their results with previous studies performed on Mg_2SiO_4, they reported that transformation rates increase with increasing iron content. They also suggested that persistence of a metastable olivine wedge to depths >660 km might be restricted to even colder and/or drier subduction zones than previously estimated. Their results are consistent with those of Hosoya et al. (2005) in that the water contents of the deeper parts of cold slabs were of the order of hundreds of wt. ppm.

On the other hand, using experimental data from Diedrich et al. (2009), Green et al. (2010) concluded that subducting oceanic plates harbor water contents of less than 100 wt. ppm. However, Diedrich et al. (2009) did not present data on compositions with water content of <300 wt. ppm. Therefore, the discussion in Green et al. (2010) pertains only to water contents ≥300 wt. ppm (Du Frane et al., 2013). Du Frane et al. (2013) presented ringwoodite growth rate measurements from olivine with a water content of ~75 wt. ppm under high *P–T* conditions. They found growth rates to be almost identical to those of olivine with a water content of ~300 wt. ppm, and significantly higher than those of nominally anhydrous olivine. They addressed the importance of enhancement by hydrolytic weakening of reaction rims, which reduces the elastic strain energy barrier to growth. They insisted that metastable persistence of olivine into the mantle transition zone would require a water content of <75 wt. ppm, indicating a considerably lower water content in slabs. However, this effect occurs easily in laboratory experiments using single crystal olivine. This is also a difficult problem because the rheology of a high-pressure phase rim and kinetics are coupled, both are time dependent, and the timescale differs between laboratory experiments and slab kinematics. Therefore, the water contents of slabs remain controversial. The *P–T* conditions of the water-content dependency of the rate for olivine–ringwoodite phase transformation with iron must be determined experimentally to discuss the water contents of the deeper portions of slabs more precisely (Kubo, personal communication).

3.3.4. Depression of the 660-km boundary

Investigating *S* to *P* converted waves, Kaneshima (2003) detected depression of the 660-km seismic discontinuity to depths of 680–690 km inside the Mariana slab, which was considered the phase boundary from ringwoodite to Pv + Mw. Here we attempt to explain this depression as a combination of depression due to the Clapeyron slope within the cold slab and that due to the kinetics associated with the ringwoodite–Pv + Mw phase transformation (Kubo et al., 2009). We calculated the depths of the 660-km phase transformation from the temperature distribution within the Mariana slab. The results show that the phase boundary is depressed to a depth of 685 km inside the slab provided that the value of the Clapeyron slope is −0.9 MPa/K, which is consistent with the seismological observations (Fig. 6). This is because in addition to the contribution from the negative Clapeyron slope whereby the temperature inside the slab is lower than that of the ambient mantle (~12 km), the effect of the kinetics that originate from the overpressure needed for phase transformation (~13 km) is added. The obtained absolute value of the Clapeyron slope is slightly larger than that reported by Kubo et al. (2009) (−0.7 MPa/K) for the Mariana slab. This is due to the temperature difference between the two models. The temperature obtained in the cold core of the Mariana slab at a depth of nearly 660 km by our model is approximately 750 °C, whereas that by Kubo et al. (2009) is 700 °C. In our model, the slab temperature was obtained using the plate cooling model, and latent heat release was calculated properly in a self-consistent manner. The slab temperature obtained using the half-space cooling model of Kubo et al. (2009) was lower than ours, and the temperature increase due to latent heat release of Kubo et al. (2009) was larger than ours, as described in Section 3.3.1. The difference in slab temperature between our model and that of Kubo et al. (2009) is greater than the temperature difference in the latent heat release between ours and that of Kubo et al. (2009), yielding a slightly larger temperature field in our study than in that of Kubo et al. (2009) in the cold core of the slab at a depth of nearly 660 km. As a result, the temperature difference between the cold core of the slab and the ambient mantle around the depth in our model is smaller than that of Kubo et al. (2009). Therefore, a larger absolute value of the Clapeyron slope is needed in our model compared to that of Kubo et al. (2009) to explain the same amount of depression of the 660-km boundary inside the Mariana slab.

The effect of latent heat absorption associated with the 660-km phase transformation, which is not included in our model, on temperature decrease and the amount of depression of the phase boundary is negligible when such a gentle Clapeyron slope is adopted. There is also a possibility that the water content anomaly between the slab and the surrounding mantle yields a depression of the 660-km phase boundary (Suetsugu et al., 2006). However, depression due to water content anomaly *h* can be given by:

Please cite this article in press as: Yoshioka, S., et al. Impact of phase change kinetics on the Mariana slab within the framework of 2-D mantle convection. Phys. Earth Planet. In. (2014), http://dx.doi.org/10.1016/j.pepi.2014.12.001

$$h = \left(\frac{\partial h}{\partial w}\right)\Delta w, \tag{21}$$

where $\frac{\partial h}{\partial w}$ is 2.7 km/wt.% (Higo et al., 2001). This indicates that even for a water content Δw of 1 wt.%, the amount of depression is 2.7 km. From this result, we conclude that the effect of the water content anomaly on depression is negligible for a water content of 250 wt. ppm for a grain size of 1 mm, as was obtained in this study.

4. Conclusions

In this study, we developed a 2-D temperature and phase calculation model associated with the subduction of an oceanic plate, by solving coupled equations for the momentum, energy, and kinetics. As a result, we obtained temperature, flow velocity, and degree of phase transformation simultaneously in a self-consistent manner as a time-marching problem. When a slab is old and subduction velocity is fast, slab temperature tends to become low, resulting in a delay of the olivine–wadsleyite phase transformation in the central part of the deep slab, producing a metastable olivine wedge. The effect of water content is included in the equation of growth rate for the olivine–wadsleyite phase transformation. The lower the water content, the deeper is the metastable olivine wedge in the cold core of the slab. The deeper the phase transformation takes place inside the slab, the larger is the latent heat release. When the phase transformation takes place at depths greater than 570 km, a temperature rise of at most 100 °C takes place in the central part of the slab due to the latent heat released. The temperature increase due to latent heat release promotes further phase transformation, causing a positive feedback effect, resulting in faster completion of phase transformation.

We applied the newly developed numerical model to the Mariana slab. Assuming that the age of the Mariana slab at the trench is 150 Myr and the subduction velocity is 9.5 cm/yr, the seismological observation that a metastable olivine wedge exists to a depth of 630 km can be well explained by water contents of 250 and 300 wt. ppm, at which nucleation takes place only along grain boundaries for grain sizes of 1 and 5 mm, respectively. If intracrystalline nucleation is considered at depths greater than 520 km, the Mariana slab needs to be drier (100 wt. ppm).

We also modeled the kinetics of the 660-km phase transformation, using the equation of the growth rate for ringwoodite to Pv + Mw. Unlike the case of the metastable olivine wedge, a metastable ringwoodite wedge cannot exist below a depth of 660 km because the temperature of the metastable domain in the phase diagram is very low (<~250 °C) (Fig. 2). We attempted to explain the seismologically determined depression of the 660-km phase boundary by 20–30 km inside the Mariana slab, using a combination of the negative Clapeyron slope under the condition of a slab temperature lower than that of the ambient mantle and the kinetics for the ringwoodite–Pv + Mw phase transformation. As a result, the amount of depression was well explained by a gentle Clapeyron slope of −0.9 MPa/K by adding the effect of kinetics resulting from the overpressure necessary for phase transformation.

Uncited references

Burnley (1995) and Rubie et al. (1992).

Acknowledgments

We thank T. Kubo for his suggestive and informative comments, and S. Kaneshima for fruitful discussion. We also thank D.A. Yuen, S.V. Sobolev, and the editor M. Jellinek for their constructive comments. All the figures were created using the Generic Mapping Tools (GMT) developed by Wessel and Smith (1998). This study was partly supported by the Grants-in-Aid for Scientific Research No. 16075207 from the Ministry of Education, Culture, Sports, Science, and Technology, Japan.

References

Akaogi, M., Takeyama, H., Kojitani, H., Kawaji, H., Atake, T., 2007. Low-temperature heat capacities, entropies and enthalpies of Mg_2SiO_4 polymorphs, and α–β–γ and post-spinel phase relations at high pressure. Phys. Chem. Miner. 34, 169–183.

Andrews, D.J., 1972. Numerical simulation of sea-floor spreading. J. Geophys. Res. 77, 6470–6472.

Avrami, M., 1941. Granulation, phase change, and microstructure kinetics of phase change. III. J. Chem. Phys. 9, 177–184.

Burnley, P.C., 1995. The fate of olivine in subducting slabs: a reconnaissance study. Am. Miner. 80, 1293–1301.

Cahn, J.W., 1956. The kinetics of grain boundary nucleated reactions. Acta Metall. 4, 449–459.

Carslaw, H.S., Jaeger, J.C., 1959. Conduction of Heat in Solids, 2nd ed. Oxford University Press, Oxford, p. 510.

Christensen, U.R., 1996. The influence of trench migration on slab penetration into the lower mantle. Earth Planet. Sci. Lett. 140, 27–39.

Christensen, U.R., Yuen, D.A., 1985. Layered convection induced by phase transitions. J. Geophys. Res. 90, 10291–10300.

Christian, J.W., 1975. The Theory of Transformations in Metals and Alloys, Part I, Equilibrium and General Kinetic Theory. Pergamon Press, Oxford.

Däßler, R., Yuen, D.A., 1996. The metastable olivine wedge in fast subducting slabs: constraints from thermo-kinetic coupling. Earth Planet. Sci. Lett. 137, 109–118.

Däßler, R., Yuen, D.A., Karato, S., Riedel, M.R., 1996. Two-dimensional thermo-kinetic model for the olivine-spinel phase transition in subducting slabs. Phys. Earth Planet. Inter. 94, 217–239.

Devaux, J.P., Schubert, G., Anderson, C., 1997. Formation of a metastable olivine wedge in a descending slab. J. Geophys. Res. 102, 24627–24637. http://dx.doi.org/10.1029/97JB02334.

Devaux, J.P., Fleitout, L., Schubert, G., Anderson, C., 2000. Stresses in a subducting slab in the presence of a metastable olivine wedge. J. Geophys. Res. 105, 13365–13373. http://dx.doi.org/10.1029/1999JB900274.

Diedrich, T., Sharp, T.G., Leinenweber, K., 2007. The effect of small amounts of H_2O on olivine to ringwoodite transformation growth rates and implications for subduction of metastable olivine. Chem. Geol. 262, 87–99.

Diedrich, T., Sharp, T.G., Leinenweber, K., Holloway, J.R., 2009. The effect of small amounts of H_2O on olivine to ringwoodite transformation growth rates and implications for subduction of metastable olivine. Chem. Geol. 262 (1–2), 87–99.

Du Frane, W.L., Sharp, T.G., Mosenfelder, J.L., Leinenweber, K., 2013. Ringwoodite growth rates from olivine with ~75 ppmw H_2O: metastable olivine must be nearly anhydrous to exist in the mantle transition zone. Phys. Earth Planet. Inter. 219, 1–10.

Fei, Y., Van Orman, J., Li, J., Van Westrenen, W., Sanloup, C., Minarik, W., Hirose, K., Komabayashi, T., Walter, M., Funakoshi, K., 2004. Experimentally determined postspinel transformation boundary in Mg_2SiO_4 using MgO as an internal pressure standard and its geophysical implications. J. Geophys. Res. 109. http://dx.doi.org/10.1029/2003JB002562.

Fukao, Y., Widiyantoro, S., Obayashi, M., 2001. Stagnant slabs in the upper and lower mantle transition region. Rev. Geophys. 39, 291–323.

Green, H.W., Cheng, W.P., Brudzinski, M.R., 2010. Seismic evidence of negligible water carried below 400-km depth in subducting lithosphere. Nature 467, 828–831.

Griggs, D.T., 1972. The sinking lithosphere and the focal mechanism of deep earthquakes. In: Robertson, E.C., Hays, J.F., Knopoff, L. (Eds.), The Nature of the Solid Earth. McGraw-Hill, New York, pp. 361–384.

Grose, C.J., 2012. Properties of oceanic lithosphere: revised plate cooling model predictions. Earth Planet. Sci. Lett. 333–334, 250–264.

Guest, A., Schubert, G., Gable, C.W., 2004. Stresses along the metastable wedge of olivine in a subducting slab: possible explanation for the Tonga double seismic layer. Phys. Earth Planet. Inter. 141, 253–267.

Higo, Y., Inoue, T., Irifune, T., Yurimoto, H., 2001. Effect of water on the spinel–postspinel transformation in Mg_2SiO_4. Geophys. Res. Lett. 28, 3505–3508.

Honda, S., 1997. Mantle dynamics II-mechanics. Iwanami-Koza Earth and Planetary Science 10 Dynamics of the Earth's Interior. Iwanami-Shoten, Tokyo, pp. 73–121 (in Japanese).

Hosoya, T., Kubo, T., Ohtani, E., Sano, A., Funakoshi, K., 2005. Water controls the fields of metastable olivine in cold subducting slabs. Geophys. Res. Lett. 32. http://dx.doi.org/10.1029/2005GL023398.

Ito, E., Takahashi, E., 1989. Postspinel transformations in the system Mg_2SiO_4–Fe_2SiO_4 and some geophysical implications. J. Geophys. Res. 94, 10637–10646.

Kaneshima, S., 2003. Small-scale heterogeneity at the top of the lower mantle around the Mariana slab. Earth Planet. Sci. Lett. 209, 85–101.

Kaneshima, S., Okamoto, T., Takenaka, H., 2007. Evidence for a metastable olivine wedge inside the subducted Mariana slab. Earth Planet. Sci. Lett. 258. http://dx.doi.org/10.1016/j. epsl.2007.03.035.

Kaneshima, S., Kubo, T., Yoshioka, S., 2012. Geophysical and mineralogical constraints on the post-spinel transformation for the Tonga slab. Phys. Earth Planet. Inter. 196–197, 23–31.

Please cite this article in press as: Yoshioka, S., et al. Impact of phase change kinetics on the Mariana slab within the framework of 2-D mantle convection. Phys. Earth Planet. In. (2014), http://dx.doi.org/10.1016/j.pepi.2014.12.001

Katsura, T., Ito, E., 1989. The system Mg_2SiO_4–Fe_2SiO_4 at high pressures and temperatures: precise determination of stabilities of olivine, modified spinel and spinel. J. Geophys. Res. 94, 15663–15670.

Katsura, T., Yamada, H., Shinmei, T., Kubo, A., Ono, S., Kanzaki, M., Yoneda, A., Walter, M.J., Ito, E., Urakawa, S., Funakoshi, K., Utsumi, W., 2003. Post-spinel transition in Mg_2SiO_4 determined by high *P–T* in situ X-ray diffractometry. Phys. Earth Planet. Inter. 136, 11–24.

Kawakatsu, H., Yoshioka, S., 2011. Metastable olivine wedge and deep dry cold slab beneath southwest Japan. Earth Planet. Sci. Lett. 303, 1–10.

Kerschhofer, L., Sharp, T.G., Rubie, D.C., 1996. Intracrystalline transformation of olivine to wadsleyite and ringwoodite under subduction zone conditions. Science 274, 79–81.

Kirby, S.H., Stein, S., Okal, E.A., Rubie, D.C., 1996. Metastable mantle phase transformations and deep earthquakes in subducting oceanic lithosphere. Rev. Geophys. 34, 261–306. http://dx.doi.org/10.1029/96RG01050.

Kubo, T., Ohtani, E., Kato, T., Urakawa, S., Suzuki, A., Kanbe, Y., Funakoshi, K., Utsumi, W., Kikegawa, T., Fujino, K., 2002. Mechanisms and kinetics of the post-spinel transformation in Mg_2SiO_4. Am. Miner. 129, 153–171.

Kubo, T., Ohtani, E., Funakoshi, K., 2004. Nucleation and growth kinetics of the α–β transformation in Mg_2SiO_4 determined by in situ synchrotron powder X-ray diffraction. Am. Miner. 89, 285–293.

Kubo, T., Ohtani, E., Kato, T., Kondo, T., Hosoya, T., Sano, A., Kikegawa, T., 2008. Kinetics of the post-garnet transformation: implications for density and rheology of subducting slabs. Phys. Earth Planet. Inter.. http://dx.doi.org/10.1016/j.pepi.2008.04.018.

Kubo, T., Kaneshima, S., Torii, Y., Yoshioka, S., 2009. Seismological and experimental constraints on metastable phase transformations and rheology of the Mariana slab. Earth Planet. Sci. Lett. 287, 12–23.

Litasov, K., Ohtani, E., Sano, A., Suzuki, A., Funakoshi, K., 2005. In situ X-ray diffraction study of post-spinel transformation in a peridotite mantle: implication for the 660-km discontinuity. Earth Planet. Sci. Lett. 238, 311–328.

Liu, M., Yund, R.A., 1995. The elastic strain energy associated with the olivine-spinel transformation and its implications. Phys. Earth Planet. Inter. 89, 177–197.

Marton, F.C., Shankland, T.J., Rubie, D.C., Xu, Y., 2005. Effects of variable thermal conductivity on the mineralogy of subducting slabs and implications for mechanisms of deep earthquakes. Phys. Earth Planet. Inter. 149, 53–64.

Mosenfelder, J.L., Marton, F.C., Ross II, C.R., Kerschhofer, L., Rubie, D.C., 2001. Experimental constraints on the depth of olivine metastability in subducting lithosphere. Phys. Earth Planet. Inter. 127, 165–180.

Perrillat, J.P., Daniel, I., Bolfan-Casanova, N., Chollet, M., Morard, G., Mezouar, M., 2013. Mechanism and kinetics of the α–β transition in San Carlos olivine $Mg_{1.8}Fe_{0.2}SiO_4$. J. Geophys. Res. 118, 110–119. http://dx.doi.org/10.1002/jgrb.50061.

Quinteros, J., Sobolev, S.V., 2012. Constraining kinetics of metastable olivine in the Marianas slab from seismic observations and dynamic models. Tectonophysics 526–529, 48–55.

Riedel, M.R., Karato, S., 1996. Microstructural development during nucleation and growth. Geophys. J. Int. 125, 397–414.

Riedel, M.R., Karato, S., 1997. Grain-size evolution in subducted oceanic lithosphere associated with the olivine-spinel transformation and its effects on rheology. Earth Planet. Sci. Lett. 148, 27–43.

Rubie, D.C., Ross, C.R., 1994. Kinetics of olivine-spinel transformation in subducting lithosphere: experimental constrains and implications for deep slab processes. Phys. Earth Planet. Inter. 86, 223–241.

Rubie, D.C., Tsuchida, Y., Yagi, T., Utsumi, W., Kikegawa, T., Shimomura, O., Brearley, A.J., 1990. An in-situ X-ray diffraction study of the kinetics of the Ni_2SiO_4 olivine-spinel transformation. J. Geophys. Res. 95, 15829–15844.

Rubie, D.C., Ross, C.R., Jackson, I., Liebermann, L.C., 1992. In: Syono, Y., Manghnani, M. (Eds.), High Pressure Research: Applications to Earth and Planetary Sciences. Terrapub, Tokyo, pp. 167–182.

Schmeling, H., Monz, R., Rubie, D.C., 1999. The influence of olivine metastability on the dynamics of subduction. Earth Planet. Sci. Lett. 165, 55–66.

Spohn, T., Hort, M., Fischer, H., 1988. Numerical simulation of the crystallization of multicomponent melts in thin dikes or sills. 1. The liquidus phase. J. Geophys. Res. 93, 4880–4894.

Stein, A.C., Stein, S., 1992. A model for the global variation in oceanic depth and heat flow with lithospheric age. Nature 369, 123–129.

Suetsugu, D., Inoue, T., Yamada, A., Zhao, D., Obayashi, M., 2006. Towards mapping the three-dimensional distribution of water in the transition zone from P-velocity tomography and 660-km discontinuity depths. In: Jacobsen, S.D., van der Lee, S. (Eds.), Earth's Deep Water Cycle. Geophysical Monograph Series, vol. 168. American Geophysical Union, pp. 237–249.

Sung, C.M., Burns, R.G., 1976. Kinetics of high pressure phase transformations: implications to the evolution of the olivine-spinel phase transition in the downgoing lithosphere and its consequences on the dynamics of the mantle. Tectonophysics 31, 1–32.

Takami, H., Kawamura, T., 1994. Finite-Difference Solutions for Partial Derivative Equations. Univ. Tokyo press, Tokyo, pp. 228 (in Japanese).

Takenaka, S., Sanshadokoro, H., Yoshioka, S., 1999. Velocity anomalies and spatial distributions of physical properties in horizontally lying slabs beneath the Northwestern Pacific region. Phys. Earth Planet. Inter. 112, 137–157.

Tetzlaff, M., Schmeling, H., 2000. The influence of olivine metastability on deep subduction of oceanic lithosphere. Phys. Earth Planet. Inter. 120, 29–38.

Tetzlaff, M., Schmeling, H., 2009. Time-dependent interaction between subduction dynamics and phase transition kinetics. Geophys. J. Int. 178, 826–844.

Torii, Y., Yoshioka, S., 2007. Physical conditions producing slab stagnation: constraints of the Clapeyron slope, mantle viscosity, trench retreat, and dip angles. Tectonophysics 445, 200–209.

Turcotte, D.L., Schubert, G., 2002. Geodynamics, 2nd ed. Cambridge Univ. Press, pp. 456.

Wang, K., Hyndman, R.D., Yamano, M., 1995. Thermal regime of the Southwest Japan subduction zone: effects of age history of the subducting plate. Tectonophysics 248, 53–69.

Wessel, P., Smith, W.H.F., 1998. New improved version of the generic mapping tools released. EOS Trans. AGU 79, 579.

Yoshii, T., 1975. Regionality of group velocities of Rayleigh waves in the Pacific and thickening of the plate. Earth Planet. Sci. Lett. 25, 305–312.

Yoshioka, S., Sanshadokoro, H., 2002. Numerical simulations of deformation and dynamics of horizontally lying slabs. Geophys. J. Int. 151, 69–82.

Yoshioka, S., Däßler, R., Yuen, D.A., 1997. Stress fields associated with metastable phase transitions in descending slabs and deep-focus earthquakes. Phys. Earth Planet. Inter. 104, 345–361.

Yu, Y.G., Wentzcovitch, R.M., Tsuchiya, T., Umemoto, K., Weidner, D.J., 2007. First principles investigation of the postspinel transition in Mg_2SiO_4. Geophys. Res. Lett. 34, L10306. http://dx.doi.org/10.1029/2007GL029462.